

## Structure–Activity and Crystallographic Analysis of a New Class of Non-amide-Based Thrombin Inhibitor

Tianbao Lu, Richard M. Soll, Carl R. Illig, Roger Bone, Larry Murphy, John Spurlino, F. Raymond Salemme and Bruce E. Tomczuk\*

3-Dimensional Pharmaceutical, Inc., Eagleview Corporate Center, Exton, PA 19341, USA

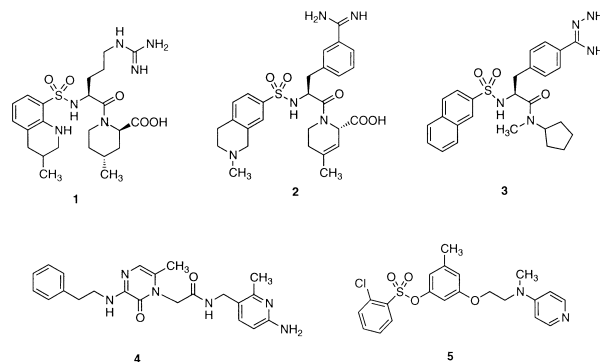
Received 3 August 1999; accepted 28 October 1999

**Abstract**—The structure–activity relationships of a novel series of non-amide-based thrombin inhibitors are described. Exploration of the P2 and the aryl binding region for this series has identified optimal groups for achieving nanomolar potency. The binding modes of these optimal groups have been confirmed by X-ray structural analysis. © 1999 Elsevier Science Ltd. All rights reserved.

The serine protease, thrombin, occupies a pivotal role in the coagulation cascade. Thrombin is involved in (1) the cleavage of fibrinogen to release fibrin, (2) the cross-linking of fibrin to form clots, (3) the stimulation of platelet aggregation, another major component of clots, and (4) the autoamplification of the coagulation cascade to produce additional active thrombin.<sup>1–3</sup> There are currently several active-site thrombin inhibitors (**1–4**) which are being pursued, with argatroban (Novastan, **1**) being the furthest in phase III development. Closely related derivatives of argatroban, such as the benzamidine UK 156406 (**2**)<sup>4</sup> and the amidrazone derivative LB-30057 (**3**)<sup>5</sup> are aminoacid-based templates. The peptidomimetic pyrazinone L-375378 (**4**) has also been reported.<sup>6</sup> We were intrigued prior to these literature reports of a non-peptide-based series exemplified by compound **5**.<sup>7</sup> This compound possessed impressive potency despite its structural simplicity, denoted by the absence of an electrophilic functionality, an aminoacid framework, and chirality. In a previous report,<sup>8</sup> we reported on **12**, an amidinopiperidine derivative related to compound **5**. Herein, we expand on the structure–activity relationships and crystallographic analysis of substitutions in the central phenyl template and in the arylsulfonate group of **11**.

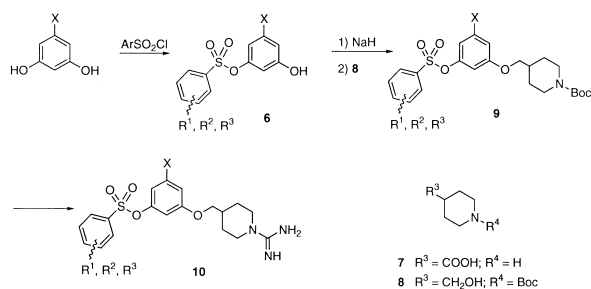
The synthesis of these amidinopiperidines is straightforward, as exemplified in Scheme 1.<sup>9</sup> The symmetrical resorcinols are monosulfonated (**6**) in good yields by using a biphasic mixture of diethyl ether and saturated

sodium bicarbonate with arylsulfonyl chlorides. The piperazine portion of the targeted compounds is derived from isonipecotic acid (**7**), which is *N*-protected (di-*t*-butyl dicarbonate (1 equiv), NaHCO<sub>3</sub> (2 equiv), dioxane:H<sub>2</sub>O (1:1), 24 h (91%)) and reduced to the alcohol **8** (BH<sub>3</sub>·THF (1 equiv), THF, 0 to 25°C (84%)). Alcohol **8** was mesylated (MsCl (1 equiv), NEt<sub>3</sub>, CH<sub>2</sub>Cl<sub>2</sub> (93%)) and coupled to the sodium salt of **6** (generated with NaH (1.1 equiv), DMF) at 50°C for 3 h (69%) to produce piperidines **9**. Alternatively, Mitsunobu coupling (PPh<sub>3</sub> (1.5 equiv), DEAD (1.5 equiv), THF, (60–85%)) was used between phenol **6** and alcohol **8** to give **9**. For analogue **30**, containing a hydroxymethyl group on the central phenyl template, the piperidine intermediate (**9**) of **27** was reduced (LiBH<sub>4</sub> (1.5 equiv), THF (61%)). Deprotection (4N HCl in dioxane, 2 h (79%)) and treatment with aminoiminomethanesulfonic acid (2 equiv, NEt<sub>3</sub>, DMF, 12 h (49%)) provided amidinopiperidines **10**. Nitroaryl derivatives **14**, **20** and **23** were reduced to anilino derivatives **15**, **21** and **24** by catalytic hydrogenation using Pd/C as a catalyst at room temperature.



**Keywords:** anticoagulants; enzyme inhibitors; substituent effects; X-ray crystal structures.

\*Corresponding author. Tel.: +1-610-458-6058; fax: +1-610-458-8249; e-mail: tomczuk@3dp.com



Scheme 1. Synthesis of amidinopiperidines.

Compounds **11–31** were evaluated for the inhibition of thrombin using standard chromogenic assays (Tables 1 and 2).<sup>10</sup> There are several structure–activity relationships in Table 1 that should be noted. First, the *para*-substitutions (**23**, **24**) are the least tolerated compared to their corresponding *meta*- and *ortho*-substituents. Second, the *meta*-substituents (**17**, **18**, **20**, **21**) are less potent than the corresponding *ortho*-substituents (**12–15**), with the exception of the 3-amino derivative (**21**) which was slightly more potent than **15**. Third, the *ortho*-substituents (**12–16**), in general, are the most potent compounds, with the exception of the 2-amino (**15**) derivative, which was the least potent compound in this group. Substitution of the 2 position with a small sampling of groups with a wide range of steric, hydrophilic, and electronic properties did not appear to be a major determinant of potency. As observed in X-ray structures (Fig. 1), the phenyl ring is found in a perpendicular stacking arrangement with Trp215 as found in this study and others.<sup>11</sup> The *ortho*-substituent is invariably directed away from the enzyme surface and is solvent exposed which would predict the non-discriminatory characteristic of this SAR.

The central phenyl template binds to the S2 region of thrombin (Table 2).<sup>12</sup> There are severe steric constraints

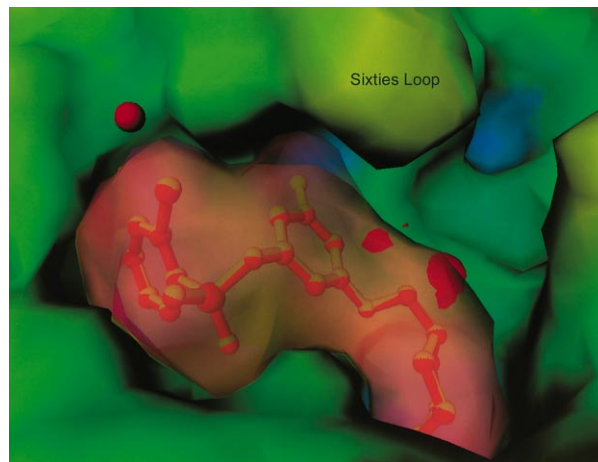
Table 1. Effects of arylsulfonate substitution

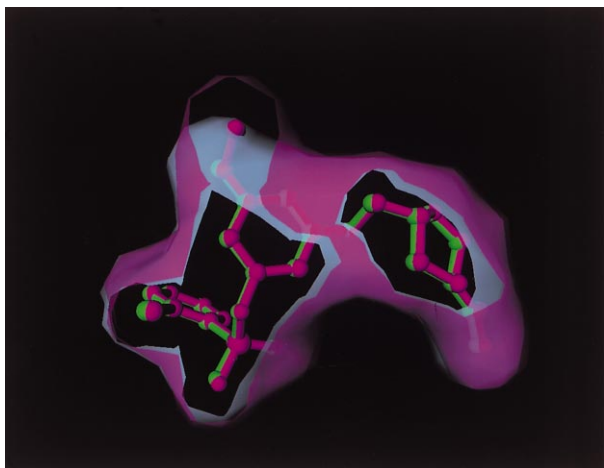
Compound	R <sup>1</sup>	R <sup>2</sup>	R <sup>3</sup>	K <sub>i</sub> thrombin (nM)
<b>11</b>	H	H	H	32 ± 2
<b>12</b>	Cl	H	H	4.6 ± 1
<b>13</b>	CF <sub>3</sub>	H	H	14 ± 1
<b>14</b>	NO <sub>2</sub>	H	H	16 ± 2
<b>15</b>	NH <sub>2</sub>	H	H	52 ± 2
<b>16</b>	CO <sub>2</sub> CH <sub>3</sub>	H	H	28 ± 1
<b>17</b>	H	Cl	H	39 ± 2
<b>18</b>	H	CF <sub>3</sub>	H	445 ± 39
<b>19</b>	H	CH <sub>3</sub>	H	36 ± 2
<b>20</b>	H	NO <sub>2</sub>	H	115 ± 11
<b>21</b>	H	NH <sub>2</sub>	H	32 ± 2
<b>22</b>	Cl	Cl	H	22 ± 1
<b>23</b>	H	H	NO <sub>2</sub>	327 ± 14
<b>24</b>	H	H	NH <sub>2</sub>	399 ± 26
<b>25</b>	-CH=CH-CH=CH-	H	H	35 ± 2

Table 2. Effects of substitutions on the central template

Compound	X	K <sub>i</sub> thrombin (nM)
<b>12</b>	CH <sub>3</sub>	4.6 ± 1
<b>26</b>	H	190 ± 11
<b>27</b>	CO <sub>2</sub> CH <sub>3</sub>	3700 ± 200
<b>28</b>	OCH <sub>3</sub>	44 ± 2
<b>29</b>	CH <sub>2</sub> CH <sub>3</sub>	39 ± 2
<b>30</b>	CH <sub>2</sub> OH	490 ± 52
<b>31</b>	Cl	30 ± 1

in this region as exemplified by the 740-fold loss of potency for the methoxycarbonyl group (**27**). On the other hand, sterically small groups such as methyl (**12**), ethyl (**29**), methoxy (**28**) and chloro (**31**) appear to be tolerated (5–44 nM), although the methyl group appears optimal. It is noteworthy to observe that minimal steric occupancy at this position, such as hydrogen (**26**) resulted in a 50-fold loss of potency versus **12**. The effect of the increased volume of the substitution under the sixties loop in the thrombin-inhibitor complex is clearly seen in the X-ray crystal structures of **12**, **26** and **29**.<sup>13</sup> There is almost no structural rearrangement of either the protein or inhibitor position seen with this substitution, although the cavity of the P2 pocket is filled by the additional volume (Fig. 1). Homologation of the methyl to an ethyl group on the central phenyl template (**29**) resulted in a decrease in potency (eightfold). Although additional volume is filled, the energy required to maintain the dihedral angle along with increased van der Waals overlap more than offsets the gain from the reduced surface exposure (Fig. 2). The close contact of the terminal CH<sub>3</sub> of the ethyl group (3.3 Å) from the imidazole ring of His57 accounts for the majority of the unfavorable energy. Additionally, the preferred angle for the dihedral angle of the ethyl substitution is 90° as compared to the observed dihedral angle of 55°, which may also contribute to the unfavorable energy.

Figure 1. X-ray structure of methyl (**12**, blue) and hydrogen (**26**, orange) on central phenyl template in thrombin.



**Figure 2.** X-ray structures of methyl (**12**, green) and ethyl (**29**, purple) on central phenyl template in thrombin.

Modeling studies of **27** in which the methoxycarbonyl group was constrained to a co-planar arrangement with the phenyl ring (presumed energy minimum) indicated a severe steric interaction with the S2 pocket of thrombin. Even when twisted 90° out of the phenyl plane, one of the oxygens of the methoxycarbonyl group is still less than 2.5 Å from the imidazole ring of His57, which is held in place by a hydrogen bonding network. The hydrogen-donating hydroxymethylene group (**30**) resulted in a 100-fold loss of potency versus **12** despite the potential for a water-mediated hydrogen bond with the enzyme in this region.

In general, compounds **11–31** showed excellent screening selectivity (0% inhibition at equal to or greater than 1 μM) against a panel of other serine proteases, including Factor Xa, plasmin, urokinase, trypsin, chymotrypsin, and elastase. The most fully characterized analogue, **12**, showed greater than 3-orders of magnitude selectivity for thrombin over these other serine proteases, as previously reported.<sup>8</sup> This selectivity against other serine proteases can be readily rationalized by docking **12** into the active sites of the published X-ray structures of Factor Xa, trypsin, and plasmin.<sup>14</sup> In Factor Xa, the replacement of Leu99 by Tyr99 within the S2 region causes a bad contact with the methyl group on the phenyl template. The structure of trypsin, which lacks the capping residues of the sixties loop and the residues for the aryl binding region, would predict the low affinity. Plasmin is even less defined in the S2 and aryl binding regions.

The present paper defines allowable groups in the present series projecting into the S2 and S3 thrombin specificity pockets. With respect to the S3 pocket, substitution of the 2 position with a small sampling of groups spanning hydrophobicity/hydrophilicity and electron donation/electron withdrawing properties affects potency the least. These results contrast the dependencies on 3-substitution and the profound effects of 4-substitution reported in earlier work.<sup>8</sup> Crystallographic analysis of **12** bound to thrombin (Fig. 1) shows that substituents *ortho* to the sulfonate linkage

are solvent exposed whereas substituents in the 3 and 4 position may clash with the protein specificity pocket. The 10-fold variance in potency within *ortho* substitution may reflect a combination of proximity to the sixties loop as well as optimal edge to face interaction with tryptophan 215.

Although there have been several reports on the use of similar aryl scaffolds in thrombin inhibitor design, limited SAR has been reported. Optimal for activity is a rigid guanidine backbone,<sup>8</sup> methyl group substitution on the orcinol, and *ortho*-substitution on the aryl sulfonate. The present data, together with our earlier work, completes the SAR on this series of potent non-peptidic, guanidino-containing compounds as it relates to *in vitro* thrombin inhibition.

### Acknowledgement

We wish to thank Stephen Eisennagel for MS and HPLC determinations as well as Mike Kolpak of US Bioscience for NMR spectra.

### References and Notes

- Colman, R. W.; Marder, V. J.; Salzman, E. W.; Hirsch, J. In *Hemostasis and Thrombosis: Basic Principles and Clinical Practice*; 3rd ed.; Coleman, R. W.; Hirsch, J.; Marder, V. J.; Salzman, E. W.; Eds.; J. B. Lippincott: Philadelphia, 1994, p 3.
- Colman, R. W.; Cook, J.; Niewiarowski, S. In *Hemostasis and Thrombosis: Basic Principles and Clinical Practice*; 3rd ed.; Coleman, R. W.; Hirsch, J.; Marder, V. J.; Salzman, E. W.; Eds.; J. B. Lippincott: Philadelphia, 1994, p. 508.
- Mann, K. G. In *Hemostasis and Thrombosis: Basic Principles and Clinical Practice*; 3rd ed.; Coleman, R. W.; Hirsch, J.; Marder, V. J.; Salzman, E. W.; Eds.; J. B. Lippincott: Philadelphia, 1994, p 184.
- Allen, M.; Abel, S. M.; Barber, C. G.; Cussans, N. J.; Danilewicz, J. C.; Ellis, D.; Hawkeswood, E.; Herron, M.; Holland, S.; Fox, D. N. A.; James, K.; Kobylecki, R. J.; Overington, J. P.; Pandit, J.; Parmar, H.; Powling, M. J.; Rance, D. J.; Taylor, W.; Shepperson, N. B. Abstracts of Papers, 215th National Meeting American Chemical Society, Dallas, TX, 1998; American Chemical Society: Washington, DC, 1998; MEDI 200.
- Lee, K.; Hwang, S. Y.; Hong, S.; Hong, C. Y.; Lee, C.-S.; Shin, Y.; Kim, S.; Yun, M.; Yoo, Y. J.; Kang, M.; Oh, Y. S. *Bioorg. Med. Chem.* **1998**, *6*, 869.
- Sanderson, P. E. J.; Lyle, T. A.; Cutrona, K. J.; Dyer, D. L.; Dorsey, B. D.; McDonough, C. M.; Naylor-Olsen, A. M.; Chen, I.-W.; Chen, Z.; Cook, J. J.; Cooper, C. M.; Gardell, S. J.; Hare, T. R.; Krueger, J. A.; Lewis, S. D.; Lin, J. H.; Lucas, B. J., Jr.; Lyle, E. A.; Lynch, J. J.; Stranieri, M. T.; Vastag, K.; Yan, Y.; Shafer, J. A.; Vacca, J. P. *J. Med. Chem.* **1998**, *41*, 4466.
- von der Saal, W.; Heck, R.; Leinert, H.; Poll, T.; Stegmeier, K.; Michel, H. WO 94/20467, 1994.
- Lu, T.; Tomczuk, B.; Illig, C. R.; Bone, R.; Murphy, L.; Spurlino, J.; Salemme, F. R.; Soll, R. M. *Bioorg. Med. Chem. Lett.* **1998**, *8*, 1595.
- Lu, T.; Illig, C. R.; Tomczuk, B.; Soll, R. M.; Subasinghe, N. L.; Bone, R. F. WO 97/11693, 1997.
- Inhibition constants were determined at 37°C in a 96-well format using a Molecular Devices plate reader. Varying

concentrations of inhibitors in 10  $\mu\text{L}$  dimethylsulfoxide were added to wells with 280  $\mu\text{L}$  of assay buffer (pH 7.5) which contained 50 mM HEPES, 0.2 M NaCl, 1% dimethylsulfoxide, 0.05% B-octyl-glucoside and substrate and incubated for 30 min at 37°C. Reactions were initiated by the addition of 10  $\mu\text{L}$  of enzyme in assay buffer without dimethylsulfoxide and substrate and the change in absorbance at 405 nm was monitored for 30 min. Apparent dissociation constants ( $K_i$  app) were obtained as the inverse slope from plots of the ratio of initial velocity in the presence of inhibitor to initial velocity in the absence of inhibitor as a function concentration. The inhibition constant ( $K_i$ ) was calculated using the equation  $K_i = K_i \text{ app}/(1 + S/K_m)$  where  $S$  is the substrate concentration  $K_m$  values for each enzyme–substrate pair were determined from

double reciprocal plots using the same final buffer buffer conditions as  $K_i$  determinations. Substrate, substrate concentration, and  $K_m$  value for human  $\alpha$ -thrombin were succinyl-Ala-Ala-Pro-Arg-*p*-nitroanilide, 100 and 320  $\mu\text{M}$ , respectively.

11. Engh, R. A.; Branstetter, H.; Sucher, G.; Eichinger, A.; Baumann, U.; Bode, W.; Huber, R.; Poll, T.; Rudolph, R.; von der Saal, W. *Structure* **1996**, *4*, 1353.

12. Bone, R.; Lu, T.; Illig, C. R.; Soll, R.; Spurlino, J. J. *Med. Chem.* **1998**, *41*, 2068.

13. Crystallographic data for **11**:  $R=20.0\%$  at 1.90 Å resolution; **26**:  $R=17.25\%$  at 2.3 Å resolution; **29**:  $R=20.5\%$  at 1.90 Å resolution. **29**:  $R=20.5\%$  at 1.90 Å resolution.

14. The X-ray structures of Factor Xa (1FAX), trypsin (1AOJ), and plasmin (1BML) are available in the Protein Database.